NUMERICAL MODELING OF UHPFRC MECHANICAL BEHAVIOR BASED ON FIBRE ORIENTATION

Sébastien Delsol (1) and Jean-Philippe Charron (2)

(1) Cima[+] Consulting Firm, Laval, Canada

(2) Polytechnique Montréal, Montréal, Canada

Abstract

The research project describes in this paper propose a methodology providing accurate prediction of the bending behavior of UHPFRC beams. The methodology comprises tensile and bending tests on UHPFRC elements, fibre orientation evaluation in those elements, and finite element calculations to reproduce the bending behaviour. An image analysis program was developed to calculate the average fibre orientation found in specimens. The program allowed the identification of correlations between UHPFRC tensile properties and fibre orientation in dogbone specimens, and the proposition of an empirical formulation. Then, bending tests and fibre orientation measurements were carried out on UHPFRC beams of various sections and reinforcements. Fibre orientations found in beams were converted in UHPFRC tensile properties with the empirical formulation. Finally, finite element calculations based on beams tensile properties led to accurate predictions of the mechanical behavior (strength and deflection) of UHPFRC beams.

Résumé

Le projet de recherche décrit dans cet article propose une méthodologie permettant de reproduire précisément le comportement flexionnel de poutres en Béton Fibré Ultra Performant (BFUP). La méthodologie comprend des essais de traction et de flexion sur spécimens en BFUP, l'évaluation de l'orientation des fibres dans ces spécimens, et des modélisations par éléments finis. Un programme d'analyse d'images a d'abord été développé pour calculer l'orientation moyenne des fibres dans le BFUP. L'utilisation du programme a permis d'établir des corrélations entre le comportement en traction directe du BFUP et l'orientation moyenne des fibres, et donc de proposer une formulation empirique du comportement en traction. Par la suite, des essais de flexion et des mesures de l'orientation des fibres ont été réalisés sur des poutres en BFUP de différentes sections et pourcentages d'armature. L'orientation moyenne des fibres mesurée dans les poutres a été convertie en lois de comportement en traction avec la formulation empirique. Enfin, les modélisations par éléments finis alimentées par ces lois de comportement ont reproduit correctement le comportement mécanique (résistance et flèche) des poutres en BFUP.

1. INTRODUCTION

Since nineties, an important research effort was dedicated to the improvement of concrete strength and durability and has led to the development of ultra-high performance fibre reinforced concrete (UHPFRC). The high homogeneity and density of the matrix, high-quality of the microstructure and addition of fibres permitted to increase significantly the compressive strength [1], tensile strength [2], post-peak ductility [3] and very low permeability and absorption [4] in comparison to normal strength concrete. Therefore, utilization of UHPFRC in structures allows partial or complete removal of reinforcement and offers exceptional durability in service.

Finite element (FE) calculations, based on characterization tests of compressive and tensile strengths of concrete and reinforcing bars, predict accurately the bending behaviour of conventional reinforced concrete structures. This is due to the fact that mechanical properties of concrete are generally similar in characterization specimens and in structures (putting aside size effect). The situation is different for fibre reinforced concrete, because fibre orientation in structures may differ from characterization specimens. As UHPFRC tensile properties vary significantly according to fibre orientation [2, 5], FE calculations can provide inappropriate prediction of the actual capacity of UHPFRC structures.

A research project was launched at Polytechnique Montreal to propose a methodology allowing accurate prediction of the bending behaviour of UHPFRC beams based on the fibre orientation measurements. The methodology is detailed in Figure 1. The first step consists to measure the uniaxial tensile properties of the UHPFRC for various fibre orientations to develop an empirical model. The second step comprises an evaluation of the bending behaviour and the fibre orientation in structural elements. The third step provides the actual UHPFRC tensile properties in structural elements from the empirical model. The last step is the determination of the bending behaviour of the structures with finite element (FE) calculations based on the actual structure tensile properties.

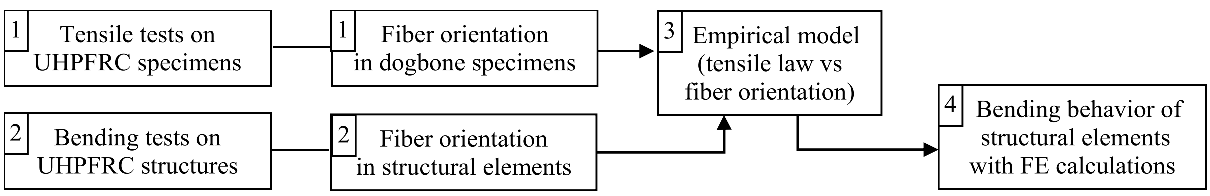

Figure 1: Proposed methodology to predict UHPFRC bending behaviour [5]

2. EXPERIMENTAL PROGRAM

2.1 Material

The UHPFRC studied in this project was a self-levelling material of water/binder ratio equals to 0.2 and containing 4%-vol. of straight steel fibres (l_f = 10 mm, ϕ_f = 0.2 mm). The material composition is listed in Table 1. Mechanical properties at 28 days are f_c = 120 MPa, f_t = 12 MPa and E_c = 36 GPa.

Table 1 : UHPFRC composition

Component	Proportion (kg/m^3)
Cement	1007
Silica Fume	252
Sand	604
Water	225
Superplasticizer	46
Fibre	312

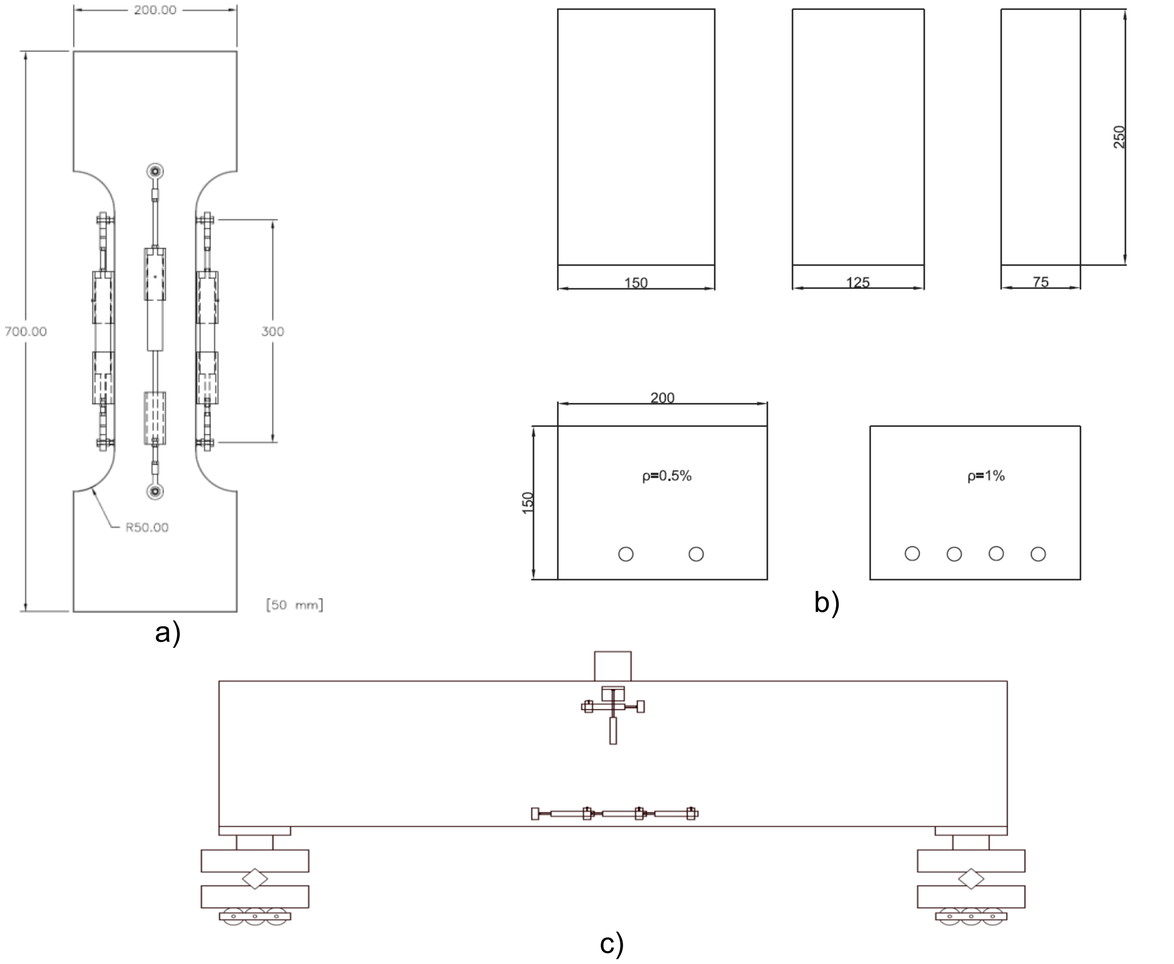

Figure 2: Test configurations, a) Dog-bone specimens, b) Beam specimens, c) Bending test

2.2 Uniaxial tensile tests

The evaluation of the UHPFRC tensile properties for various fibre orientations was obtained on dog-bone shape specimens (Figure 2a) cast with a procedure adapted from [6]. Six specimens of four different theoretical fibre orientations were produced. Specimens were tested under uniaxial tension, cut near the failure zone and then analyzed with a program to obtain the fibre orientation. The tensile tests were carried out with a 2.5 MN load frame. The loading rate was controlled in displacement at a speed of 0.1 mm/min in the pre-peak phase, the speed was progressively increase to 1 mm/min in the post-peak phase.

2.3 3-points bending tests

Bending tests were completed on 1.1 m UHPFRC beams of various sections and reinforcement ratios ranging from 0 to 1 % (Figure 2b). The beams were filled manually with a recipient as described by [7] to orientate fibres mainly in the beam longitudinal axis. The testing configuration is illustrated in Figure 2c. The centered force was applied by a 240 kN actuator and beams were supported by rollers allowing rotation and longitudinal displacements at each extremity. The loading rate was 0.2 mm/min. At the end of the test, the beams were cut near the failure zone and then specimens were analyzed with a program to obtain the fibre orientation.

2.4 Image analysis

The image analysis procedure developed in the project consists to extract a specimen in a structure by saw cutting or core drilling, polish it to obtain a smooth and straight surface, and paint the specimen surface to highlight fibres in the concrete. Then the studied surface is digitalized at 2400 dpi resolution with a scanner and analysed with a in-house program. The program applies to the image a morphologic filter and a global threshold to identify accurately fibre outline and defects, then a Hough transform determines characteristics of ellipses formed by each fibre cross-section in the matrix. The ellipse characteristics (centroids, dimensions) detected for each fibre allow calculations of the fibre orientation in comparison to the studied surface. The fibre orientation considered in this project represents the average orientation measured in specimen cross-sections under analysis. The number of fibres used in the evaluation of the orientation is typically 4 000 fibres and 35 000 fibres for dogbone and beam specimens respectively. More details can be found in [5]. Figure 3 presents the image evolution processed by the program, from digitalization, binearization and fibre detection.

The detection capability of the program is above 97 % of fibres in a digitalized image. Its accuracy to calculate the fibre angle was established by analysing perfect and truncated ellipses with known orientation. Figure 4 shows the program error in degree according to the real orientation angle of truncated fibres. The accuracy on the fibre angle can vary from 75 % (error of 22º on a fibre oriented at 0º) to 99 % (error less than 1º on a fibre oriented at 80º). On a UHPFRC section where multiple fibre orientations are found, the average fibre orientation varies typically from 30 to 50º in beams specimens (which means that the majority of fibres are within this range of orientation). In this range of orientation, Figure 4 indicates that the program provides an accuracy of ± 2º on the fibre orientation. This variability of ± 2º on results of the fibre orientation will be considered later on in finite element calculations.

a)

b)

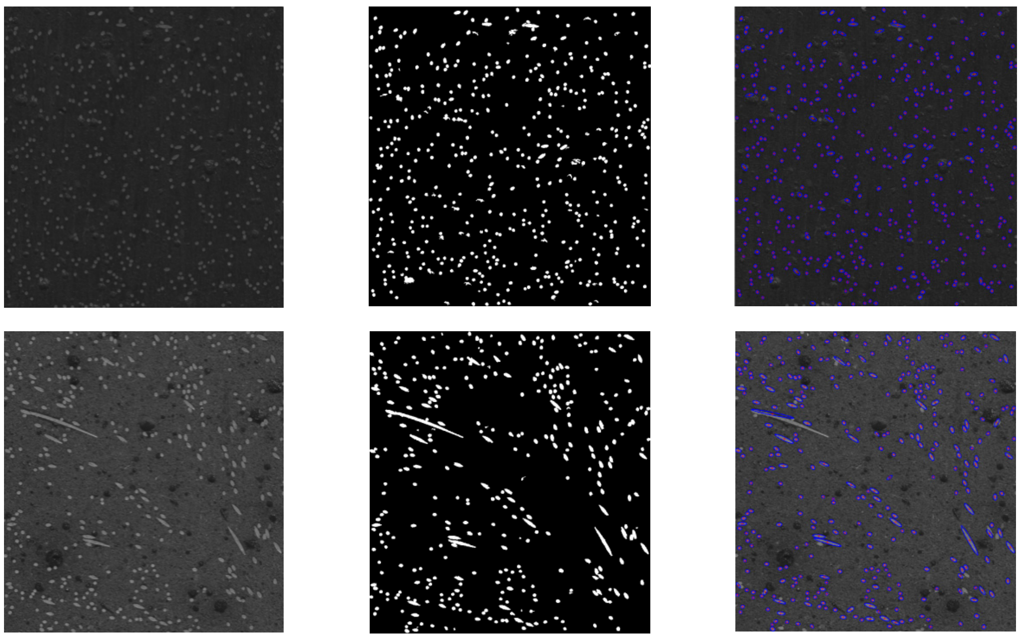

Figure 3 : Image evolution from digitalization, binearization to fibre detection for,
a) Unreinforced beam specimen, b) Reinforced beam specimen

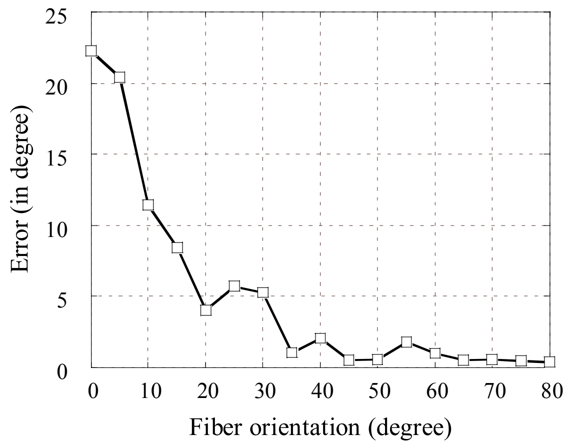

Figure 4 : Average error of the orientation angle on truncated ellipses digitilized at 2400 dpi

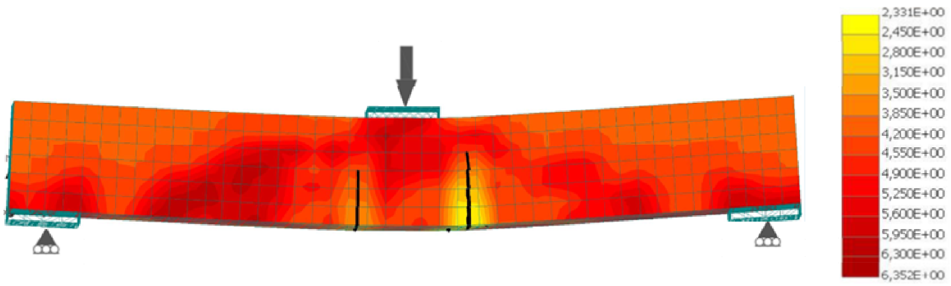

Figure 5 : Numerical model, mesh and support conditions for a reinforced beam FE model (legend shows the principal stresses in MPa, stress field presented at ultimate load)

2.5 Finite element calculations

Nonlinear finite element analyses were performed with Atena 3D software [8] to reproduce the bending behaviour of beams. Material laws specifically adapted to hardening and softening concrete as UHPFRC are available in the software. The tensile law uses Menétrey-William surface failure and compressive law uses Rankine failure criterion. The numerical model developed for the project is illustrated in Figure 5. The mesh comprises brick elements in longitudinal sections and tetrahedral elements at supports. The boundary conditions and load application in the model reproduce experimental conditions.

3. RESULTS AND DISCUSSION

3.1 Uniaxial tensile behavior

Figure 6 presents the UHPFRC uniaxial tensile behaviour according to the average fibre orientation measured in the dog-bone specimens. A fibre at 0º is considered parallel to the tensile principal stresses, whereas a fibre at 90º is perpendicular to principal stresses in the dog-bone specimens. Experimental results show that the slope and length of the hardening phase are reduced with increasing the fibre angle. A reduction in length of 95 % and in ultimate strength of 60 % are noted with the most unfavourable fibre orientation 54º. The general trend of the softening phase is similar for various fibre orientations, the strength reduction at an equivalent crack opening being almost proportional to the ultimate strength obtained in each configuration. Unlike Osterlee's observation [2], UHPFRC tensile stiffness was not modified by fibre orientation variation.

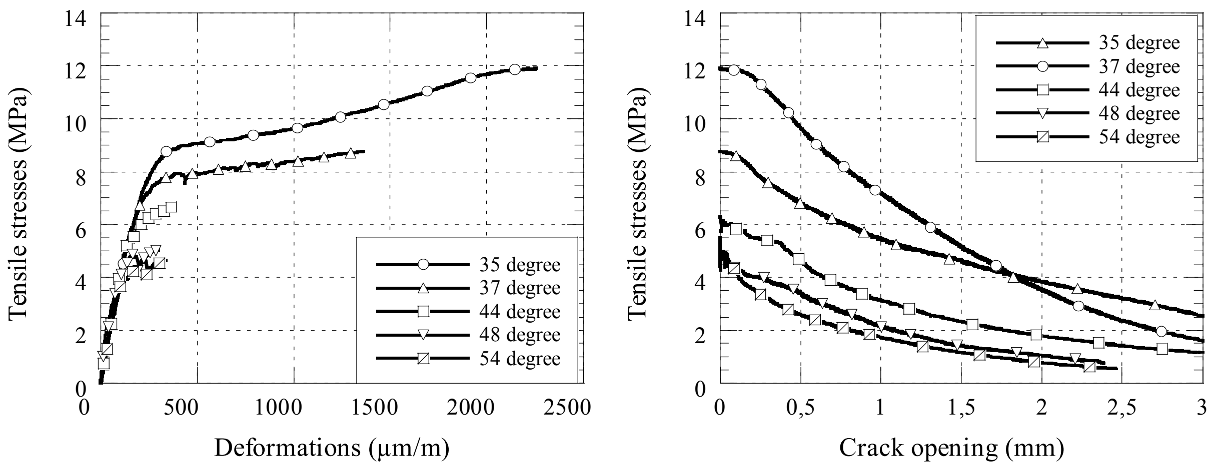

Figure 6 : UHPFRC uniaxial tensile behavior according to the average fibre orientation, a) Pre-peak, b) Post-peak

3.2 Empirical tensile model

An empirical tensile model was developed to provide the UHPFRC uniaxial tensile behaviour from the average fibre orientation measured in specimens or structural elements made with the same materials. The empirical model is based on correlations described in Section 3.1 and relies only on fibre orientation. Trial models based on fibre density or a combination of fibre orientation and density in the UHPFRC did not provide better predictions in this project involving one material composition (Table 1).

The tensile empirical model adopts the nomenclature and basic form proposed by [9], the model is illustrated in Figure 7 and equations are detailed in Table 2. The pre-peak tensile behaviour is described by three points, two points if the fibre orientation is above 47º. The post-peak behaviour is described by Redaelli's equation [10], which was modified to take into account fibre orientation.

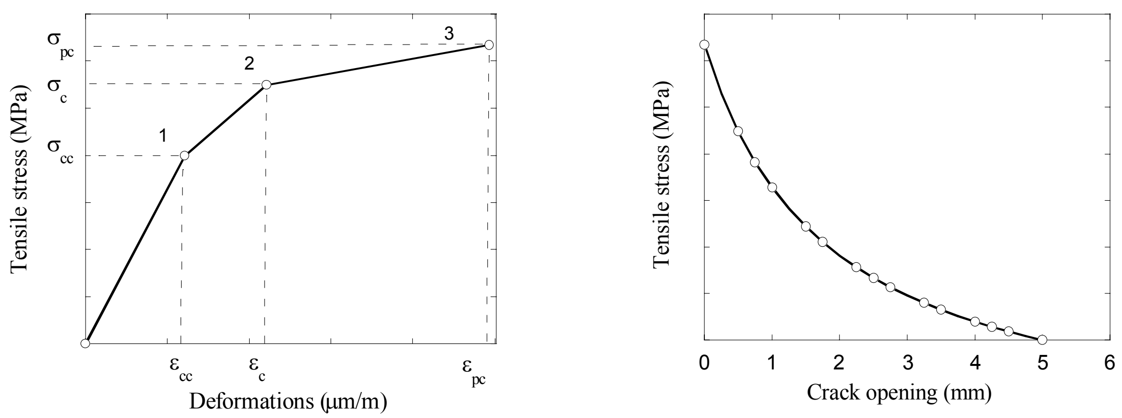

Figure 7: Empirical tensile model, a) Pre-peak behavior, b) Post-peak behavior

Figure 8 shows comparison of the experimental curves and theoretical tensile behaviours provided by the empirical model (Table 2) for the average fibre orientations measured in dog-bone specimens. The empirical model provides an accurate reproduction of the UHPFRC hardening and softening phases, a precision of 96 % and 94 % is attained for each phase respectively. High accuracy of the experimental model is explained by the fact that the experimental results were used to develop the model. However, the model will be shortly validated with results of other experimental programs, and also adapted to consider fibre density when using UHPFRC with different fibre dosages.

Table 2: Equations of the empirical tensile model based on the average fibre orientation

Pre-peak	$\sigma_{cc} = \begin{cases} 50{,}18 \cdot \cos\theta - 35{,}38, & \theta < 37° \\ 2{,}79 \cdot \cos\theta + 2{,}28, & \theta \geq 37° \end{cases}$	$\varepsilon_{cc} = \frac{\sigma_{cc}}{E_c} = \frac{\sigma_{cc}}{36000}$
	$\sigma_c = \begin{cases} 55{,}79 \cdot \cos\theta - 37{,}27, & \theta < 38° \\ 19 \cdot \cos\theta - 8{,}4, & 47° \geq \theta \geq 38° \end{cases}$	$\varepsilon_c = \begin{cases} [62 \cdot (\sigma]_c - 3{,}128), & \theta < 38° \\ 929 \cdot \cos\theta - 511, & 47° \geq \theta \geq 38° \end{cases}$
	$\sigma_{pc} = \begin{cases} 172 \cdot \cos\theta - 128{,}69, & \theta < 37° \\ 20 \cdot \cos\theta - 7{,}23, & 54{,}5° \geq \theta \geq 37° \end{cases}$	$\varepsilon_{pc} = \begin{cases} \frac{\sigma_{pc} - 4{,}551}{0{,}0031}, & \theta < 37° \\ 6698 \cdot \cos\theta - 4120, & 47° \geq \theta \geq 37° \\ 300, & 54{,}5° \geq \theta \geq 47° \end{cases}$
Post-peak	$\sigma(w) = \frac{\sigma_{pc}}{1 + \left(w / 1 + \cos\theta\right)} \left(\frac{l_f / 2 - w}{l_f / 2} \right)$	- l_f: Fibre length (mm) - w : Crack opening (mm) - θ : Average fibre orientation (°) - σ_{cc}, σ_c, σ_{pc}, ε_{cc}, ε_c, ε_{pc}: see Figure 7

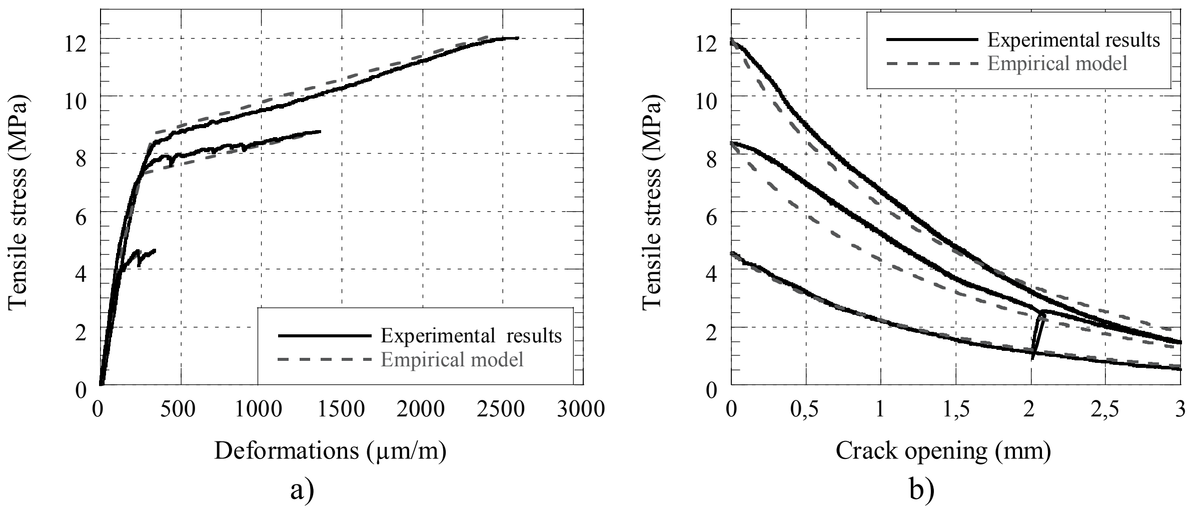

Figure 8: Empirical tensile model and test results, a) Pre-peak behavior, b) Post-peak behavior

3.3 Bending behavior

The experimental program included bending tests on UHPFRC beams of various sections and reinforcement ratios (Figure 2b). Experimental results obtained in two tests are analysed in the next sections, for an unreinforced beam of 150 mm width and 250 mm depth (Figure 9a), and for a reinforced beam of 200 mm width and 150 mm depth with a reinforcement ratio of 0.5% (Figure 9b). Experimental results demonstrated that the linear elastic phase was followed by a hardening phase with multiple microcrack at beams bottom section, then a macrocrack developed near the ultimate load, and the failure occurred at the macrocrack location. As expected, the reinforced beam presented more ductility after the achievement of the ultimate load.

3.4 Finite element calculations

Reproduction of the bending behaviour of UHPFRC beams was done with the finite element model described in Section 2.5. The UHPFRC uniaxial tensile law considered in the model were obtained from the methodology described in Figure 1. Cut samples were first taken near failure location of beams and were analysed with the in-house program (Section 2.4). Then, the average fibre orientation provided by the program was introduced in the empirical tensile model to calculate the theoretical tensile behaviour (Section 3.2). Figure 10 presents the tensile behaviour retrieved from the methodology applied on dog-bone specimens submitted to a uniaxial tensile test and beams submitted to bending tests. Although a similar casting procedure was used to fill all specimens, a significant variability is observed in the tensile laws. The smaller cross-section of the dog-bone specimens favoured orientation of fibres parallel to principal stresses and led logically to the highest tensile properties and strongest strain hardening phase. Fibres were less oriented parallel to principal stresses in beams longitudinal axis, particularly in presence of reinforcing bars which disrupted UHPFRC flow in the formwork. Difference of fibre orientation in unreinforced and reinforced beams can be clearly observed in Figure 3. As a consequence, the lowest tensile properties and shortest strain hardening phase were obtained in the reinforced beams.

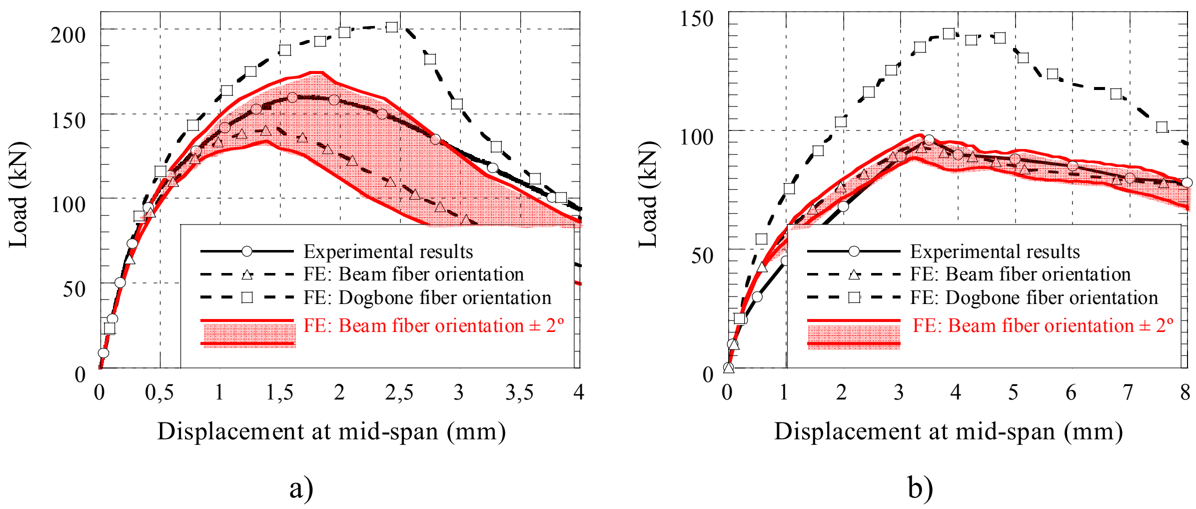

Figure 9: Experimental and theoretical (FE calculations) bending behavior of UHPFRC beams, a) Unreinforced beam (w = 150 mm, d = 250 mm),
b) Reinforced beam (w = 200 mm, d = 150 mm, ρ = 0.5 %)

Comparison of FE calculations and experimental results of UHPFRC beams tests are shown in Figure 9. Four curves of FE calculations are presented. Calculations taking into account the tensile properties calculated in the dog-bone specimens demonstrate clearly that fibre orientation in dog-bone specimens overestimates the ultimate strength by 25 % and the mid-span deflection by 56 % in comparison to experimental results.

However, calculations based on the actual fibre orientation in beams provide a better estimation of beams strength and ductility. For unreinforced beams, calculations underestimate by 8 % the ultimate strength and by 33 % the mid-span deflection (average values). For reinforced beams, calculations underestimate by 1% the ultimate strength and by 13 % the mid-span deflection (average values).

Residual discrepancies between experimental results and FE calculations based on the actual beam fibre orientation are mainly related to error of the image analysis program. As mentioned in Section 2.4, an overall accuracy of ± 2º is expected on the average fibre orientation measured in a specimen. Considering this limitation, FE calculations were done also with beam fibre orientation ± 2º. These calculations are represented by the upper and lower limits of the red shade area in Figure 9. The experimental curves of the unreinforced and reinforced UHPFRC beams are found within the prediction area provided by the FE calculations.

The previous observations confirm the importance to estimate the structural behaviour of beams with consideration of the actual fibre orientation and tensile properties in beams to obtain accurate FE predictions. Introducing tensile properties found in characterization specimens (dog-bone specimens) in FE calculation may lead to significant overestimation of strength and deflection of beams, which represent unconservative evaluations. In this context, the methodology adopted in this research project is relevant to improve accuracy of FE calculations used for design and evaluation of UHPFRC structural elements.

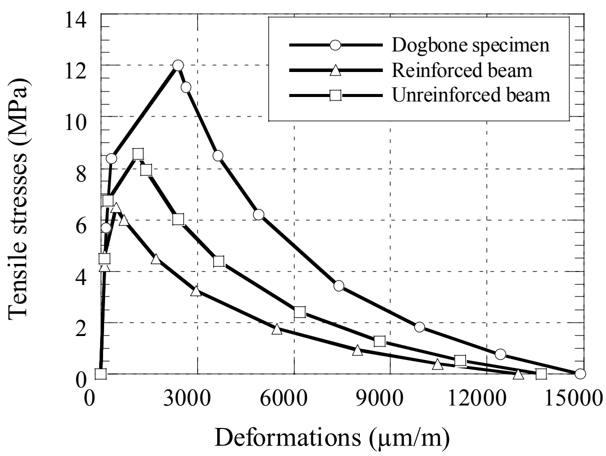

Figure 10: UHPFRC tensile laws calculated with the fibre orientation and the empirical model, and later introduced in the FE calculations

4. CONCLUSIONS

A research project was launched at Polytechnique Montreal to propose a methodology providing accurate prediction of the bending behaviour of UHPFRC beams based on fibre orientation measurements. The methodology comprises tensile and bending tests on UHPFRC elements and fibre orientation evaluation to reproduce the bending behaviour with FE calculations. Analysis of results leads to the following conclusions:

- The slope and length of UHPFRC hardening phase are reduced with increasing the fibre orientation angle. Reductions in length of 95 % and in ultimate strength of 60 % are noted with the most unfavourable fibre orientation.
- The in-house image analysis program detects above 97 % of fibres in a section and its accuracy on the fibre angle measurement varies according to the fibre orientation. For UHPFRC section where multiple fibre orientation is found, the program should provide an accuracy of ±2º on the average fibre orientation.

- The tensile empirical model provides an accurate reproduction of the UHPFRC hardening and softening phases based on the average fibre orientation. The model will be shortly validated with other experimental results, and also adapted to consider various fibre dosages in the UHPFRC.
- Bending behaviour of UHPFRC beams reproduce with FE calculations based on dog-bone specimens fibre orientation over evaluate significantly beams strength and deflection. Introducing tensile properties corresponding to the actual beam fibre orientation clearly improve accuracy of FE calculations to predict strength and deflection of beams, particularly if the variability of fibre orientation measurement is considered.
- The proposed methodology to reproduce the UHPFRC bending behaviour was validated on beams of various sections and reinforcement ratios. The methodology is relevant to improve accuracy of FE calculations used for design and evaluation of UHPFRC structural elements.

ACKNOWLEDGEMENTS

The research project was financially supported by the Natural Science and Engineering Research Council of Canada (NSERC). Moreover, some materials were provided free of charge by Bekaert, Euclid, Holcim and Tech-Mix.

REFERENCES

[1] Mansur, M. (1999). Stress-Strain Relationship of High-Strength Fibre Concrete in Compression. *J. Mater. Civ. Eng., 11*(1), 21.

[2] Oesterlee, C. (2010). *Structural Response of Reinforced UHPFRC and RC Composite Members*, Ph.D. thesis Ecole Polytechnique Fédérale de Lausanne.

[3] Naaman, A. E., & Reinhardt, H. (2006). Proposed classification of HPFRC composites based on their tensile response. *Materials and Structures, 39*(5), 547-555.

[4] Charron, J.P., Denarie, E., Bruhwiler, E. (2008). Transport Properties of Water and Glycol in an Ultra High Performance Fibre Reinforced Concrete (UHPFRC) Under High Tensile Deformation. Cement and Concrete Research, 38(5), p. 689-698.

[5] Delsol, S. (2012). *Évaluation du coefficient d'orientation des fibres dans les bétons renforcés de fibres métalliques*, M.Sc. thesis École Polytechnique de Montréal.

[6] Hannant, D. J., & Spring, N. (1974). Steel-Fibre-Reinforced motar: a techenique for producing composites with uniaxial fibre aligment. *Mag. of Concrete Research, 26*(Compendex), 47-48.

[7] Markovic, I. (2006). *High-performance hybrid-fibre concrete: development and utilisation* Ph.D. thesis Delft University.

[8] Cervenka, V., Jendele, L., & Cervenka, J. (2011). *Atena Program Documentation* (Vol. 1: Theory). Prague.

[9] Naaman, A. E. (2008). High Performance Fibre Reinforced Cement Composites. in Shi & Mo, (Éds.), *High-Performance Construction Materials - Science and Applications*: World Scientific.

[10] Redaelli, D. (2009). *Comportement et modélisation des éléments de structure en béton fibré à ultra-hautes performances avec armatures passives*, Ph.D. thesis, EPFL, Lausanne